Marine Biology Research, 2012; 8: 163–171

ORIGINAL ARTICLE

Latitudinal variability (6°S–20°N) of early summer phytoplankton species compositions and size-fractioned productivity from Java Sea to South China Sea

GANG LI[1], LIANGMIN HUANG[1], HUAXUE LIU[1], ZHIXIN KE[1], QIANG LIN[1], GUANGYAN NI[2], JIANQIANG YIN[1], KAIZHI LI[1], XINGYU SONG[1], PINGPING SHEN[1] & YEHUI TAN[1]*

[1]*Key Laboratory of Marine Bio-resources Sustainable Utilization, South China Sea Institute of Oceanology, CAS, Guangzhou, Guangdong, China, and* [2]*Key Laboratory of Vegetation Restoration and Management of Degraded Ecosystems, South China Botanical Garden, CAS, Guangzhou, Guangdong, China*

Abstract

In order to study the effects of latitudinal change in physical and chemical environments on phytoplankton cells, we investigated the early summer phytoplankton biomass, species composition and size-fractioned productivity in surface water from the Java Sea to the South China Sea (from 6°S to 20°N) from 18 May to 27 May 2010. Chlorophyll *a* (Chl *a*) concentration decreased latitudinally from 0.18 (~6°S) to 0.05 μg l^{-1} (~10°N). The dominant species, the cyanobacteria *Trichodesmium erythraeum*, dinoflagellates (e.g. *Gyrodinium dominans*, *Amphidinium carterae* and *Gonyaulax* spp.) and diatoms (e.g. *Thalassionema nitzschioides*, *Rhizosolenia* spp. and *Chaetoceros* spp.) changed to only the dinoflagellate species. Also, the Chl *a* biomass increased to 0.14 μg l^{-1} towards the end of the survey (~20°N) with the dinoflagellates as the most abundant group. Productivity of phytoplankton assemblages coincided with Chl *a* concentration, and decreased accordingly from 9.24 ± 0.71 to 2.87 ± 0.41 μg C l^{-1} day^{-1}, then increased to 5.45 ± 1.1 μg C l^{-1} day^{-1}. Chl *a* concentration and productivity were significantly correlated ($P < 0.05$) with microplankton cell abundance, as well as nutrient concentrations, which appeared to exert a strong influence over latitudinal variation in primary production.

Key words: *Carbon fixation, latitudinal variation, phytoplankton, size distribution*

Introduction

Marine phytoplankton plays an important role in the oceanic biological CO_2 pump, resulting in continuous dissolution of CO_2 from the atmosphere into the oceans. These autotrophic organisms sustain the largest ecosystems on the earth, accounting for less than 1% of photosynthetic biomass, but contributing to about half of primary production on our planet (Field et al. 1998). According to Pianka (1966), any spatial or temporal variations in phytoplankton biomass, community structure or productivity would be an important feature in regulating the marine ecosystems; therefore, many researchers have focused on such dynamics of phytoplankton assemblages (Marañón et al. 2001; Eilertsen & Frantzen 2007; Li et al. 2009; Li et al. 2011a).

Several factors have been identified as being responsible for the dynamics of phytoplankton species in the oceans (Eilertsen & Frantzen 2007). Light intensity can be a crucial environmental factor by driving or photoinhibiting algal photosynthesis, and thus controlling growth or production (Colern 1999; Gao et al. 2007a, b), while vertical mixing impacts a series of physiological responses to solar radiation (Helbling et al. 2003; Li et al. 2009) and further alters their community structure (Eilertsen & Frantzen 2007). Temperature regulates ocean surface stratification and reduces the exchange of nutrients between the deeper nutrient-rich waters

*Correspondence: Yehui Tan, Key Laboratory of Marine Bio-resources Sustainable Utilization, South China Sea Institute of Oceanology, CAS, Guangzhou, Guangdong, 510301, China. E-mail: tanyh@scsio.ac.cn

Published in collaboration with the University of Bergen and the Institute of Marine Research, Norway, and the Marine Biological Laboratory, University of Copenhagen, Denmark

(Accepted 4 June 2011; Published online 31 January 2012; Printed 10 February 2012)

ISSN 1745-1000 print/ISSN 1745-1019 online © 2012 Taylor & Francis
http://dx.doi.org/10.1080/17451000.2011.615323

and the surface waters. A reduction in nutrient delivery from the deep ocean can significantly alter phytoplankton species composition in the surface waters (Chen & Chen 2006). In some cases, the availability of trace metals (mainly iron) can also result in the variability of phytoplankton standing stock or size distribution (Helbling et al. 1991; Coale et al. 1996). Changes in the physical (e.g. temperature, light penetration and mixing) and chemical (e.g. nutrients and trace metals) environments are known to influence the phytoplankton communities (Helbling et al. 1991, 2003; Li et al. 2009, Li et al. 2011b; Qiu et al. 2010). These factors mostly likely change latitudinally from the Java Sea to the South China Sea. The biomass or size distribution as well as production of phytoplankton would thus change accordingly in this area; however, few studies have documented such geographical changes.

The marginal area of the Java Sea to South China Sea covers the equatorial and subtropical regions (>30 latitudinal degrees from 6°S to 24°N) and supports millions of people living along the coasts based on its fishery and other natural resources (Morton & Blackmore 2001). It also plays a potentially important role in regulating the global climate change (Qu et al. 2009). In recent years, extensive studies on physical oceanographic processes have been performed in this area (see the review by Qu et al. 2009 and literature therein). To the best of our knowledge, however, little is known about its marine biota and ecology, especially the latitudinal dynamics of phytoplankton, even though a few studies have been conducted in some limited areas, such as Xisha and Zhongsha Islands (Cheng & Liu 1997), Nansha Islands (Huang 1991; Huang & Chen 1997; Yang & Jiao 2004), the central basin (Liu et al. 2007) and the coastal (Gin et al. 2000; Song et al. 2009) or pelagic waters (Ning et al. 2004; Chen & Chen 2006, Li et al. 2011a). Moreover, there have been few latitudinal studies that have measured the species composition and size structure of the community or its activity. Here, we showed the latitudinal dynamics of phytoplankton species, size-fractioned production as well as nutrient concentrations [i.e. dissolved inorganic nitrogen (NO_3^-, NO_2^-) and phosphate (PO_4^{3-})] in surface waters from the Java Sea to the South China Sea (6°S to 20° N).

Materials and methods

Study area and sampling protocol

This study was carried out during a cruise from 18 May to 27 May 2010 from Sunda Strait (Java Sea) to northern South China Sea (Figure 1), which covered about 26 latitudinal degrees (6°S to 20°N) with the water depth varying from 30 to 3000 m. Surface seawater samples (up to 20 cm depth) were obtained every morning (8:30) and evening (21:30) using a 5-l acid-cleaned (1 mol l^{-1} HCl) polycarbonate bucket with a cap. The water samples were collected at an interval of approximately 2 latitudinal degrees and were used immediately (within 15 min) for determination of size-fractioned photosynthetic carbon fixation, chlorophyll *a*, species composition, nutrients, as well as temperature and salinity as described below.

Determination of photosynthetic carbon fixation

To determine the rate of photosynthetic carbon fixation, the water samples were pre-filtered through 200-μm pore-size mesh (to remove large zooplankton), divided into triplicate 500-ml polycarbonate tubes (Nalgene®), inoculated with 400 μl of 4 μCi (0.148 MBq) $NaH^{14}CO_3$ solution (ICN Radiochemicals, USA) and incubated beneath the surface (5 cm) of a shade-free water tank in which the temperature was controlled within a range of 30–32°C [the same range as sea-surface temperature (SST)] by continuously pumping surface seawater. The incubations were exposed to solar radiation and lasted for 24 h. Additional duplicate tubes wrapped in black foil were incubated as the dark control. After the incubation, the cells were sequentially filtered onto 20- and 3-μm pore-size polycarbonate filters (25 mm, Osmonics Inc.) and a 0.7-μm pore-size glass fibre filter (25 mm, Whatman GF/F), which was immediately frozen and stored at –20°C for later analysis. The frozen filter was placed into a 20-ml scintillation vial, thawed and inoculated with 0.5 ml of 0.5 mol l^{-1} HCl, and left uncapped for 24 h in a fume hood to expel non-fixed ^{14}C. Scintillation cocktail (5 ml) was added to each vial and radioactivity was measured with a liquid scintillation counter (LS 6500, Beckman Coulter, USA). The photosynthetic carbon fixation was calculated according to the JGOFS ^{14}C-protocol (Knap et al. 1996). A total of 14 incubations were performed during the survey.

Chlorophyll a and species analyses

At the beginning of each experiment, chlorophyll *a* (Chl *a*) concentration of three cell-size fractions was determined by sequentially filtering 800 ml of surface seawater onto 20-, 3- and 0.7-μm filters described above, which were then wrapped in aluminum foil and stored at –20°C for later extraction and measurement. Chl *a* concentration was determined by fluorescence with a Turner Design 10 fluorometer following the equations of Parsons et al.

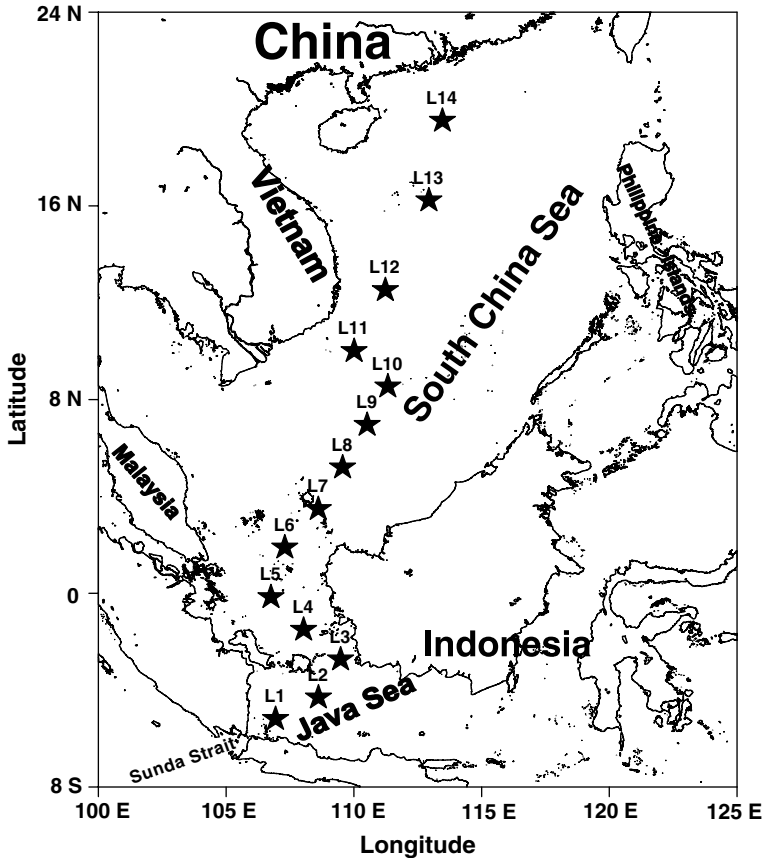

Figure 1. Map of the South China Sea and Java Sea, with the stars (*) showing the sampling sites where the experiments were performed from 18 May to 27 May 2010.

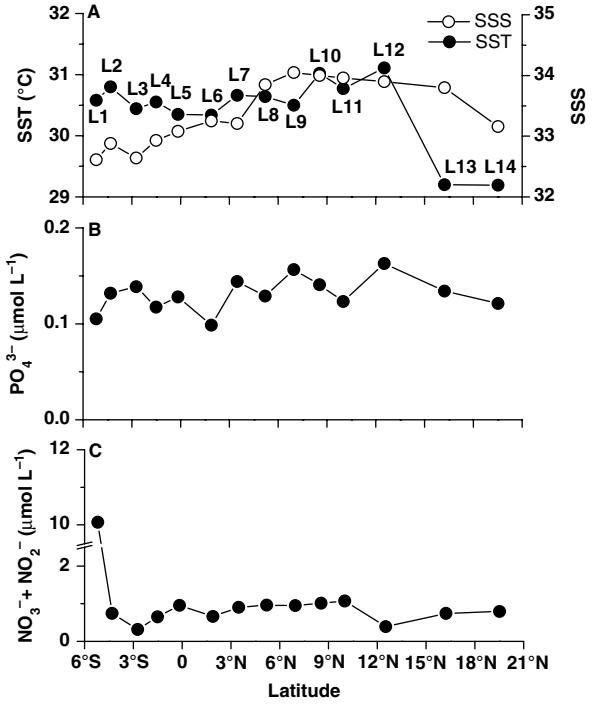

Figure 2. Latitudinal variations (from 6°S to 20°N) in (A) surface seawater temperature (SST, °C) and salinity (SSS), and concentrations of (B) PO_4^{3-} and (C) $NO_3^- + NO_2^-$ in μmol l^{-1} during the cruise.

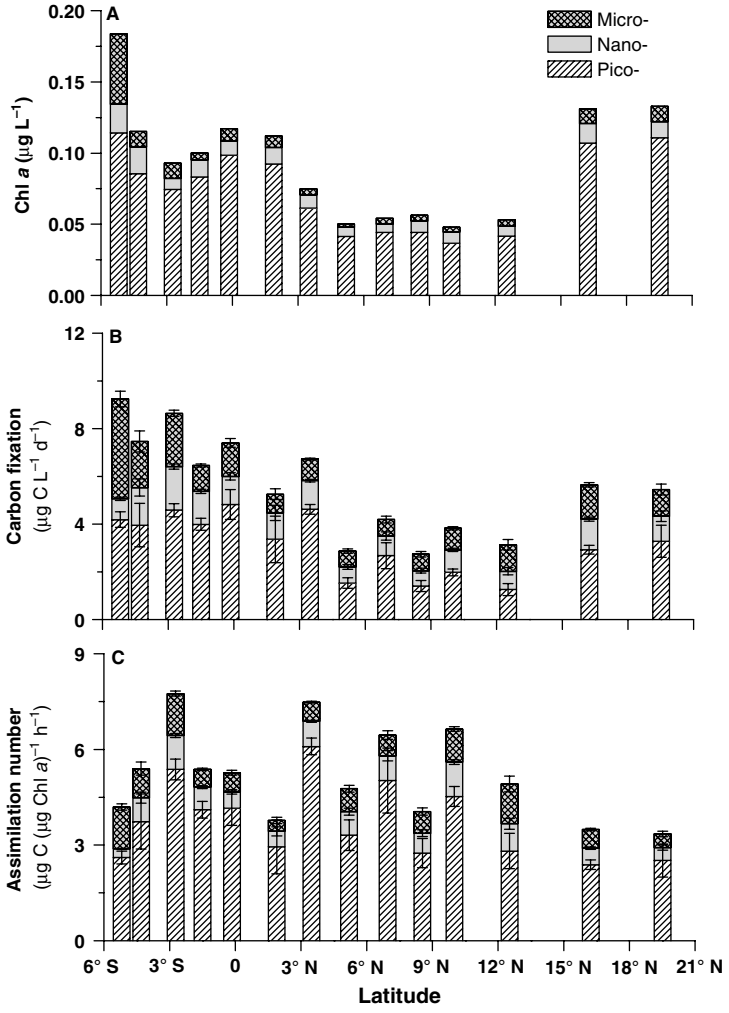

Figure 3. Biological characteristics in surface seawater from 6°S to 20°N: (A) Chl *a* biomass (μg l^{-1}) of micro- (> 20 μm), nano- (3–20 μm) and pico-plankton (< 3 μm); (B) carbon fixation (μg C l^{-1} day^{-1}); and (C) assimilation number [μg C (μg Chl *a*)$^{-1}$ h^{-1}] of three cell-size fractions. Vertical bars represent the standard deviations ($n = 3$).

(1984). After complete extraction with 90% acetone (v/v) in the dark for 24 h at 4°C, total Chl *a* was obtained by adding together the three size fractions. In this article, phytoplankton larger than 20 μm cell-diameter was defined as microplankton, 3–20 μm as nanoplankton and 0.7–3 μm as picoplankton.

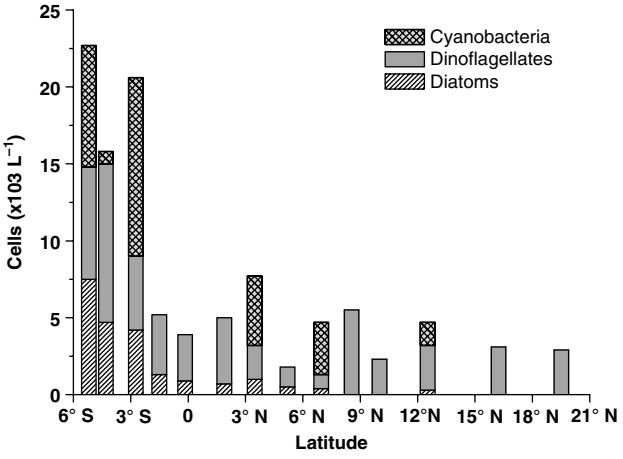

Figure 4. Variability of surface phytoplankton community structure from the Java Sea to the South China Sea.

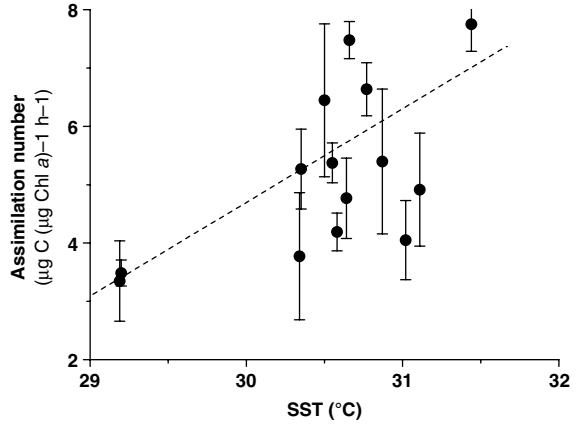

Figure 5. Photosynthetic rate [µg C (µg Chl *a*)$^{-1}$ h^{-1}] as a function of the SST (°C), with the dashed line representing the significant relationship ($r = 0.76$, $p < 0.01$, $n = 14$). Vertical bars represent the standard deviations ($n = 3$).

For species analysis, phytoplankton samples were fixed with Lugol's solution according to Parsons et al. (1984). The subsample of 800 ml was concentrated down to 20 ml by settling for at least 24 h and siphoning the supernatant, then qualitative and quantitative analyses were carried out with a compound microscope for the whole 0.5 ml sample using Utermöhl's (1958) method.

Measurements of environmental factors

For nutrient measurements, the water sample was pre-filtrated through a Whatman GF/F filter, and concentrations of nitrate (NO_3^-), nitrite (NO_2^-), phosphate (PO_4^{3-}) and silicate (SiO_3^{2-}) were analysed with a nutrients autoanalyser (Quickchem 8500, Lachat Instruments, USA) following the description of Kirkwood et al. (1996). This equipment has detection limits of 0.014, 0.005 and 0.075 µmol l^{-1} for $NO_3^- + NO_2^-$, PO_4^{3-} and SiO_3^{2-}, respectively. It was calibrated regularly with the support of the manufacturer against CSK standard solutions, and also calibrated before and during the measurements of each of the eight samples. Analyses of errors were less than 10%; the silicate concentrations were not reported here due to the contamination by glass fibre filters.

Surface seawater temperature (SST) and salinity (SSS) were measured with a multi-parameter water quality monitor SONDE (YSI 6600, Yellow Springs Instruments, USA) during the cruise.

Statistics

Mean and standard deviations were calculated and the correlation between variables was established using a Kendall's t test with 95% confidence limit.

Results

Surface seawater salinity (SSS) increased latitudinally from 32.61 at L1 station ($\sim 6°$S) to 34.05 at L9 station ($\sim 8°$N), then decreased gradually to the end of the survey to 33.16 at L14 station ($\sim 20°$N) (Figure 2A). SST showed the same trend as SSS, with the values gradually increasing from 30.58 (L1) to 31.11°C (L12), then sharply decreasing to 29.14°C (L14) (Figure 2A). Phosphate concentrations increased northwards from 0.10 to 0.16 µmol l^{-1} (Figure 2B). Dissolved inorganic nitrogen ($NO_3^- + NO_2^-$) concentration also displayed a high geographical variability, with the maximum and minimum being 10.0 and 0.39 µmol l^{-1} at station L1 and L12, respectively (Figure 2C).

Latitudinal variations in phytoplankton biomass (Chl *a*) and size distributions throughout the investigation are shown in Figure 3. The highest Chl *a* concentration of 0.18 µg l^{-1} was observed at L1 station, which sharply decreased to 0.09 µg l^{-1} at L3 station, then to 0.05 µg L^{-1} at L8 station (Figure 3A). The lower Chl *a* appeared at L8 to L12 station where concentrations ranged from 0.048 to 0.053 µg l^{-1}; however, it sharply increased to 0.14 µg l^{-1} at L14 station (Figure 3A). Higher concentrations of Chl *a* (e.g. L1 station) were observed in near-shore waters (Figure 3A), indicating the influence of land-derived runoffs. In most cases, picoplankton (0.7–3 µm) accounted for 80% of Chl *a* allocation (0.04–0.12 µg Chl *a* l^{-1}) (Figure 3A). The Chl *a* of nanoplankton (3–20 µm) appeared to be more stable and varied within a narrow range of 0.01–0.02 µg l^{-1} (Figure 3A); while that of microplankton (>20 µm) varied greatly from 0.002 to 0.05 µg l^{-1} and decreased from L1 station northwards (Figure 3A). Chl *a* biomass of micro-cells was positively correlated to total Chl *a* ($r = 0.79$, $P < 0.01$) (Table II), indicating

the micro-cells dominated the overall variations of total phytoplankton. The peak of Chl *a* (e.g. L1 station) also had the highest phytoplankton abundance ($\sim 2.1 \times 10^4$ cells l^{-1}), with the cyanobacteria *Trichodesmium erythraeum*, dinoflagellates *Gyrodinium dominans*, *Amphidinium carterae* and *Gonyaulax* spp. and diatoms *Thalassionema nitzschioides*, *Rhizosolenia* spp. and *Chaetoceros* spp. being the dominant species (Table I, Figure 4). Interestingly, the diatoms species gradually disappeared from L1 station northwards (Figure 4), with the dinoflagellates becoming the dominant groups, and the cyanobacteria, *T. erythraeum* being dominant at some stations (L1, L3, L7, L9, Table I, Figure 4).

Carbon fixation by phytoplankton assemblages was also variable, and coincided well with Chl *a* biomass (Figure 3A, B). The photosynthetic capacity per volume of seawater sharply decreased from 9.24 ± 0.71 (L1) to 2.87 ± 0.41 μg C l^{-1} day^{-1} (L8), but then gradually increased to 5.45 ± 1.1 μg C l^{-1} day^{-1} (L14) at the end of the survey (Figure 3B). Total daily productivity was generally higher at stations in the vicinity of land (e.g. L1 to L6). Carbon fixation of three cell-size fractions to total productivity displayed a similar pattern as that of Chl *a*: i.e. picoplankton represented the most important contributors, accounting for 45–69% of the daily primary production; whereas micro- and nano-fractions contributed to 14–45% and 10–25%, respectively (Figure 3B). Moreover, Chl *a* of micro-cells was positively correlated ($r = 0.59$, $P < 0.05$) to total carbon fixation (Table II), reflecting the contribution of micro-cells on total primary production. Finally, photosynthetic rate ranged from 3.78 ± 1.1 (L6) to 7.75 ± 0.45 μg C (μg Chl *a*)$^{-1}$ h^{-1} (L3), with micro-, nano- or pico-cells accounting for an average of 13, 15 and 72%, respectively (Figure 3C).

When the phytoplankton biomass and productivity were plotted against the environmental factors (i.e. SST, SSS, NO_2^- and NO_3^- and PO_4^{3-}), the biomass and production (Chl *a* and C-fixation) were negatively ($P < 0.05$) correlated to SSS, but positively correlated ($P < 0.05$) to the concentration of NO_3^- and NO_2^- (Table II), which indicated that the primary production was to some extent controlled by the available nutrients derived from the land. On the other hand, there was a positive relationship ($r = 0.76$, $P < 0.01$) between photosynthetic rate and SST (Figure 5), suggesting the higher temperature favoured the photosynthetic capacity of phytoplankton assemblages.

Discussion

In this study, we demonstrated the spatial variability over 26 latitudinal degrees for biomass, species compositions and productivity of phytoplankton from the Java Sea to the South China Sea. We observed a decrease in Chl *a* from 6°S to 8°N and an increase in Chl *a* from 8°N to 20°N, as well as a change in the dominant phytoplankton species from cyanobacteria, diatoms and dinoflagellates to only dinoflagellates. Productivity of phytoplankton showed the same pattern with Chl *a* concentration for the whole transact.

High surface salinity and temperature often characterize the equatorial regions of the world's oceans (Bryan et al. 1974), the values of which, however, were lower in the equatorial zone (i.e. 6°S to 3°N) of the present study (Figure 2A). The land-derived runoffs could be responsible for the lower salinity as the sampling sites were located close to the land (Figure 1). Variations in surface temperature are often regulated by solar energy, especially in the ocean region in this study, where the severe stratification prevails in summer (Chen & Chen 2006). Unfortunately, solar irradiance or dose for the experimental periods was not obtained due to no radiometer being available. Nevertheless, according to our observations, the presence of cloudy days at the beginning (18, 20 May) or end (26, 27 May) of the survey might have accounted for their lower SST (Figure 2A). The sampling time (morning and evening) could be another cause for the SST variations. The river inputs from Pearl River and upwelling might also be responsible for the lower SST at L13 and L14 stations (Yin et al. 2001; Voss et al. 2006). Temperature can affect all biochemical reactions catalysed by enzymes in phytoplankton cells (Gillooly et al. 2001), and impact the primary productivity (Laubscher et al. 1993; Husa et al. 2008; Montagnes et al. 2008). Higher temperature would increase the activity of enzymes involved in photosynthetic processes, resulting in higher CO_2 assimilation rates (Figure 5) and, subsequently, the growth of phytoplankton assemblages (Eilertsen & Frantzen 2007; Bissinger et al. 2008).

The drastic latitudinal variation was seen in the decrease (6°S to 6°N) and following increase (6°N to 20°N) of phytoplankton biomass or production (Figure 3A,B) as well as the contrasting changes of the dominant species (Figure 4, Table I). Macronutrients such as phosphate or nitrate often modulate phytoplankton abundance and size distributions in marine ecosystems (Yin et al. 2001; Ning et al. 2004; Ryan et al. 2008). In our study area, the concentration of phosphate was relatively high (0.10–0.16 μoml l^{-1}) (Figure 2C) and most likely did not limit phytoplankton growth (Wu et al. 2003). Nitrogen was less than 1.0 μoml l^{-1} in most cases (Figure 2C) and was even sometimes undetectable (Gong et al. 1992), leading to the low

Table I. Latitudinal variability of the dominant species from L1 (~6°S) to L14 station (~20°N) in $\times 10^3$ cells l^{-1} during the cruise. Blank indicates no algal cells were observed for the special species.

Species composition	Stations												
	L1	L2	L3	L4	L5	L6	L7	L8	L9	L11	L12	L13	L14
Diatoms													
Bacteriastrum spp.	0.2	0.9		0.1									
Chaetoceros spp.	1.0	0.8	0.5	0.3	0.4		0.5						
Coscinodiscus spp.	0.2	0.1	1.0	0.2									
Diploneis sp.	0.2												
Ditylum sol (Grunow) De Toni, 1894	0.1												
Guinardia flaccida (Castracane) Peragallo, 1892	0.2												
Lauderia annulata Cleve, 1873	0.1				0.1								
Leptocylindrus danicus Cleve, 1889		0.1											
Mastogloia rostrata Hustedt, 1933	0.1						0.1						
Pleurosigma aestuarii (Brébisson *ex* Kützing) W. Smith, 1853	0.1	0.1											
Pleurosigma angulatum (Queckett) W. Smith, 1852	0.1												
Pseudo-nitzschia delicatissima (P.T. Cleve, 1897) Heiden, 1928	0.9												
Rhizosolenia spp.	1.4	0.6	1.1	0.2			0.1	0.1	0.2			0.1	
Skeletonema costatum (Greville) Cleve, 1873			0.3			0.6							
Helicotheca tamesis Ricard, 1987		0.2											
Thalassionema nitzschioides (Grunow) Mereschkowsky, 1902	1.0	1.0	0.2	0.1	0.2			0.2					
Thalassiosira sp.	0.1	0.3		0.2	0.2	0.1	0.2	0.1					
Thalassiothrix longissima Cleve & Grunow, 1880	0.2											0.1	
Dinoflagellates													
Alexandrium spp.	0.1	0.1	0.1			0.6	0.2			0.2	0.2	0.1	0.2
Amphidinium carterae Hulbert, 1957	0.3	0.7	0.8	1	0.2	0.6	0.7	0.2	0.1	0.6	0.8	0.4	0.3
Ceratium spp.	0.2	0.2								0.1			0.1
Dinophysis sp.		0.1											0.1
Gonyaulax ovalis Schiller, 1929	0.2	0.5	0.2			0.2	0.1	0.1	0	0.1	0.1		0.2
Gonyaulax spp.	2.0	3.0	1.1	0.9	0.3	0.8	0.4	0.8	0.2	2.0	0.6	0.7	0.7
Gyrodinium dominans Hulbert, 1957	4.1	4.7	2.2	1.7	2.0	1.6	0.3	0.2	0.4	2.0	0.2	1.0	0.7
Heterodinium sp.		0.1		0.1			0.1					0.1	
Prorocentrum spp.	0.2	0.8	0.3	0.1	0.5	0.3	0.2		0.2	0.3	0.4	0.6	0.4
Protoperidinium sp.	0.1						0.1			0.1			
Pyrocystis noctiluca J. Murray, 1885 *ex* Haeckel, 1890	0.1												
Pyrodinium sp.										0.1			0.2
Scrippsiella trochoidea (Stein) Balech *ex* Loeblich III, 1965		0.1	0.1	0.1		0.2	0.1						0.2
Cyanobacteria													
Trichodesmium erythraeum Ehrenberg	7.9	0.8	11.6				4.5		3.4			1.5	
Total	21	15	20	4.7	3.8	4.9	7.3	1.7	4.4	5.4	2.3	4.4	2.9

Redfield ratio (N:P) (i.e. 2.3:8.7, except L1). Phytoplankton growth may be limited by nitrogen in this region because the N:P ratio is less than 16:1, resulting in the low primary production (Figure 3B). A consequence of low nitrogen concentrations and a high N:P ratio is the dominance of the diazotroph *Trichodesmium erythraeum*, which can outcompete other phytoplankton cells due to their ability to fix dinitrogen gas in regions of low fixed nitrogen concentrations (Voss et al. 2006; Subramaniam et al. 2008). Besides the changes in nutrients regimes, the salinity seemed to regulate the community shifts as well, as shown in the higher diatom abundance with lower SSS (Figure 2A and 4). The grazing pressure could also contribute to the observed community changes (Montagnes et al. 2008). The trace metals (e.g. iron) could be another cause for the variability in standing stock or community structure through powering the blooms of the larger cells (Helbling et al. 1991; Coale et al. 1996). In summer, the study area was strongly stratified (Chen & Chen 2006); the land-derived runoffs could be the main sources of nutrients, which enhanced the nutrient concentrations and primary production, indicated by the negative correlation of the SSS and Chl *a* or carbon fixation (Table II).

Cell size is one of the important factors influencing the phytoplankton cells distribution or community structure, as it determines their metabolic and growth rates (Raven & Kübler 2002). In this study, small cells accounted for the bulk of the phytoplankton, with picoplankton (0.7–3 μm) occupying 80% and 56% of the productivity based on Chl *a* or CO_2 fixation (Figure 3A, B), which was consistent with the previous reports in this ocean area (Huang 1991; Ning et al. 2004) or others (Coale et al. 1996;

Table II. *r* and *p* values of total Chl *a* (μg l^{-1}) or carbon fixation (μg C l^{-1} day^{-1}) plotted against the micro-cells Chl *a* (μg l^{-1}) and environmental factors [i.e. SST (°C), SSS, $NO_3^- + NO_2^-$ (μmol l^{-1}) and PO_4^{3-} (μmol L^{-1})] during the cruise. The stars (⋆) represent the significant difference.

	SST		SSS		DIN		PO_4^{3-}		SiO_3^{2-}	
	r	*p*	*r*	*p*	*r*	*p*	*r*	*p*	*r*	*p*
Chl *a*	–0.52	0.056	–0.72	0.012⋆	0.61	0.019⋆	–0.62	0.018⋆	–0.03	0.92
C-fixation	–0.19	0.51	–0.92	0.001⋆	0.53	0.048⋆	–0.38	0.194	0.31	0.28

Marañón et al. 2001). Picoplankton is often quantitatively important both in terms of biomass and productivity in open oceans (Figure 3A), as compared to coastal or estuarine waters (Tremblay & Legendre 1994). The small cells with a large surface per unit volume can utilize nutrients more efficiently under low nutrient conditions (Raven & Kübler 2002), and thus successfully dominate the oligotrophic oceans (Figure 3A). Moreover, the abundance of micro-cells was positively ($P < 0.05$) correlated to total phytoplankton biomass or productivity (Table II), suggesting that the phytoplankton in larger cells mainly contributed to the geographical variations of the total phytoplankton productivity.

Acknowledgements

We are very thankful for the comments and suggestions of two anonymous reviewers and of Subject Editor Dr David J.S. Montagnes that helped to improve our manuscript. This work was supported by Key Innovation Group Project of Chinese Academy of Sciences (KZCX2-YW-Q07), National Natural Science Foundation (41130855), Natural Science Foundation of Guangdong (S2011040000151), National Project of Sciences and Technology (2008FY110100), CAS Strategic Pilot Science and Technology (XDA05030403)".(XDA05030403)". and MEL Young Scientist Visiting Fellowship of State Key Laboratory of Marine Environment Science, Xiamen University (MELRS 1006). Thanks are also given to Qiuyan Lin for species analysis, to Yongqiang Chen and Dajun Qiu for experimental assistance and to captain and crews of the research ship *Shiyan I* for logistic support.

References

Bissinger JE, Montagnes DJS, Sharples J, Atkinson D. 2008. Predicting marine phytoplankton maximum growth rates from temperature: Improving on the Eppley curve using quantile regression. Limnology and Oceanography 53:487–93.

Bryan K, Manaber S, Pacanowski RC. 1974. A global ocean–atmosphere climate model: Part II. The oceanic circulation. Journal of Physical Oceanography 16:30–46.

Chen YL, Chen HY. 2006. Seasonal dynamics of primary and new production in the northern South China Sea: The significance of river discharge and nutrient advection. Deep Sea Research 53:971–86.

Cheng Z, Liu S. 1997. Marine diatoms of Xisha Islands, South China Sea III: One new species of *Mastogloia* and five new species records of other genera. Tropical Oceanology 16:88–90. (in Chinese with English abstract)

Coale KH, Johnson KS, Fitzwater ST, Gordon RM, Tanner S, Chavez FP, et al. 1996. A massive phytoplankton bloom induced by an ecosystem-scale iron fertilization experiment in the equatorial Pacific Ocean. Nature 383:495–501.

Colern JE. 1999. The relative importance of light and nutrient limitation of phytoplankton growth: A simple index of coastal ecosystem sensitivity to nutrient enrichment. Aquatic Ecology 33:3–16.

Eilertsen HC, Frantzen S. 2007. Phytoplankton from two sub-Arctic fjords in northern Norway 2002–2004: I. Seasonal variations in chlorophyll a and bloom dynamics. Marine Biology Research 3:319–32.

Field CB, Behrenfeld MJ, Randerson JT, Falkowski P. 1998. Primary production of the biosphere: Integrating terrestrial and oceanic components. Science 281:237–40.

Gao K, Li G, Helbling EW, Villafañe VE. 2007a. Variability of UVR effects on photosynthesis of summer phytoplankton assemblages from a tropical coastal area of the South China Sea. Photochemistry and Photobiology 83:802–09.

Gao K, Wu Y, Li G, Wu H, Villafañe VE, Helbling EW. 2007b. Solar UV-radiation drives CO2-fixation in marine phytoplankton: A double-edged sword. Plant Physiology 144:54–59.

Gillooly JF, Brown JH, West GB, Savage VM, Charnov EL. 2001. Effects of size and temperature on metabolic rate. Science 293:2248–51.

Gin KY-H, Lin X, Zhang S. 2000. Dynamics and size structure of phytoplankton in the coastal waters of Singapore. Journal of Plankton Research 22:1465–84.

Gong G, Liu KK, Liu C, Pai S. 1992. The chemical hydrography of the South China Sea west of Luzon and a comparison with the west Philippine Sea. Terrestrial. Atmospheric and Oceanic Sciences 3:587–602.

Helbling EW, Gao K, Goncalves RJ, Wu H, Villafañe VE. 2003. Utilization of solar UV radiation by coastal phytoplankton assemblages off SE China when exposed to fast mixing. Marine Ecology Progress Series 259:59–66.

Helbling EW, Villafañe VE, Holm-Hansen O. 1991. Effects of iron on productivity and size distribution of Antarctic phytoplankton. Limnology and Oceanography 36:1879–85.

Huang L. 1991. A preliminary study on the distribution of photosynthetic pigments and primary production in the sea area of Nansha Islands. In Chen Q, editor. Collected Papers on Marine Biology Study of Nansha Islands and the Adjacent Sea Areas (II). China Ocean Press, Beijing: p 34–47. (in Chinese)

Huang L, Chen C. 1997. Distribution of chlorophyll *a* and primary productivity of Nansha Islands sea area in winter. In Chen Q, Huang L, editors. A Study on Ecological Processes of

Nansha Islands Sea Area (I). Beijing: Science Press, p 1–15. (in Chinese)

Husa V, Sjøtun K, Brattenborg N, Lein TE. 2008. Changes of macroalgal biodiversity in sublittoral sites in southwest Norway: Impact of an introduced species or higher temperature? Marine Biology Research 4:414–28.

Knap A, Michaels A, Close A, Ducklow H, Dickson A, editors., 1996. Protocols for the Joint Global Ocean Flux Study (JGOFS) Core Measurements, JGOFS Report No. 19, Reprint of the IOC manuals and guides No. 29, UNESCO 1994, p 43–90.

Kirkwood DS, Aminot A, Carlberg SR. 1996. The 1994 quasimeme laboratory performance study: Nutrients in seawater and standard solutions. Marine Pollution Bulletin 32:640–45.

Laubscher RK, Perissinotto R, McQuaid CD. 1993. Phytoplankton production and biomass at frontal zones in the Atlantic sector of the Southern Ocean. Polar Biology 13:471–81.

Li G, Wu Y, Gao K. 2009. Effects of typhoon Kaemi on coastal phytoplankton assemblages in the South China Sea, with special reference to the effects of solar UV radiation. Journal of Geophysical Research 114:G04029, doi:10.1029/2008JG000896.

Li G, Gao K, Gao G. 2011a. Differential impacts of solar UV on photosynthetic carbon fixation from the coastal to offshore surface waters in the South China Sea. Photochemistry and Photobiology 87:329–34.

Li G, Gao K, Yuan D, Zheng Y, Yang G. 2011b. Relationship of photosynthetic carbon fixation with environmental changes in the Jiulong River estuary of the South China Sea, with special reference to the effects of solar UV radiation. Marine Pollution Bulletin 62:1852-8.

Liu H, Chang J, Tseng CM, Wen LS, Liu KK. 2007. Seasonal variability of picoplankton in the Northern South China Sea at SEATS station. Deep Sea Research 54:1602–16.

Marañón E, Holligan PM, Barciela R, González N, Mouriño B, Pazló MJ, et al. 2001. Patterns of phytoplankton size structure and productivity in contrasting open-ocean environments. Marine Ecology Progress Series 216:43–56.

Montagnes DJS, Morgan G, Bissinger JE, Atkinson S, Weisse T. 2008. Short-term temperature change may impact freshwater carbon flux: A microbial perspective. Global Change Biology 14:2823–38.

Morton B, Blackmore G. 2001. South China Sea. Marine Pollution Bulletin 42:1236–63.

Ning X, Chai F, Xue H, Cai Y, Liu C, Shi J. 2004. Physical–biological oceanographic coupling influencing phytoplankton and primary production in the South China Sea. Journal of Geophysical Research 109:C10005, doi:10.1029/2004JC 002365.

Parsons TR, Maita Y, Lalli CM. 1984. A Manual of Chemical and Biological Methods for Seawater Analysis. Toronto: Pergamon Press, p 1–173.

Pianka ER. 1966. Latitudinal gradients in species diversity: A review of concepts. The American Naturalist 100:33–46.

Qiu D, Huang L, Zhang J, Lin S. 2010. Phytoplankton dynamics in and near the highly eutrophic Pearl River Estuary, South China Sea. Continental Shelf Research 30:177–86.

Qu T, Song YT, Yamagata T. 2009. An introduction to the South China Sea throughflow: Its dynamics, variability and application for climate. Dynamics of Atmospheres and Oceans 47:3–14.

Raven JA, Kübler JE. 2002. New light on the scaling of metabolic rate with the size of algae. Journal of Phycology 38:11–16.

Ryan NJ, Mitrovic SM, Bowling LC. 2008. Temporal and spatial variability in the phytoplankton community of Myall Lakes, Australia, and influences of salinity. Hydrobiologia 608:69–86.

Song X, Huang L, Zhang J, Huang H, Li T, Su Q. 2009. Harmful algal blooms (HABs) in Daya Bay, China: An in situ study of primary production and environmental impacts. Marine Pollution Bulletin 58:1310–18.

Subramaniam A, Yager PL, Carpenter EJ, Mahaffey C, Björkman K, Cooley S, et al. 2008. Amazon River enhances diazotrophy and carbon sequestration in the tropical North Atlantic Ocean. Proceedings of the National Academy of Sciences 105:10460–65.

Tremblay JE, Legendre L. 1994. A model for the size-fractionated biomass and production of marine phytoplankton. Limnology and Oceanography 39:2004–14.

Utermöhl H. 1958. Toward the improvement of the quantitative phytoplankton method. Mitteilungen-Internationale Vereiningung fur Limnologie 9:1–38.

Voss M, Bombar D, Loick N, Dippner JW. 2006. Riverine influence on nitrogen fixation in the upwelling region off Vietnam, South China Sea. Geophysical Research Letter 33:L07604, 4 pages.

Wu J, Chung SW, Wen LS, Liu KK, Chen LL, Chen HY, et al. 2003. Dissolved inorganic phosphorus, dissolved iron, and Trichodesmium in the oligotrophic South China Sea. Global Biogeochemical Cycles 17:1008.

Yang Y, Jiao N. 2004. Dynamics of picoplankton in Nansha Islands area of the South China Sea. Acta Oceanologica Sinica 23:493–504.

Yin K, Qian PY, Wu MCS, Chen JC, Huang L, Song X, et al. 2001. Shift from P to N limitation of phytoplankton growth across the Pearl River estuarine plume during summer. Marine Ecology Progress Series 211:17–28.

Editorial responsibility: David Montagnes

Copyright of Marine Biology Research is the property of Taylor & Francis Ltd and its content may not be copied or emailed to multiple sites or posted to a listserv without the copyright holder's express written permission. However, users may print, download, or email articles for individual use.